Semidilute solutions of poly(methacrylic acid) in the absence of salt: Dynamic light-scattering study

M. Sedlák*, Č. Koňákt, P. Štěpánek and J. Jakeš
Institute of Macromolecular Chemistry, Czechoslovak Academy of Sciences, Heyrovsky Sq. 2, 162 06 Prague 6, Czechoslovakia
(Received 14 July 1986)

Water solutions of poly(methacrylic acid) of molecular weight $M_w = 3.0 \times 10^4$ and $M_w = 4.0 \times 10^5$, neutralized with NaOH, were investigated by photon correlation spectroscopy. At a low degree of neutralization α, the short-time decay only is observed. When $\alpha > 0$, a second, much slower, process becomes noticeable. It gains quickly in influence when α increases. The reciprocal values of characteristic relaxation times for both dynamic processes were found to decrease linearly with the square of the scattering vector, showing that both processes are diffusive. The following interpretation of these processes founded on the concentration and angle dependences of the corresponding diffusion coefficients and scattering amplitudes is given: (1) for the low-molecular-weight sample ($M_w = 3.0 \times 10^4$), D_f (fast process) can be attributed to the Nernst–Hartley diffusion coefficient of polyions, and D_s (slow process) to a diffusion of interchain domains (clusters) with a radius of gyration $R_G \approx 50$ nm; (2) for the high-molecular-weight sample ($M_w = 4.0 \times 10^5$), where an overlap of polymer chains occurs, D_f can be attributed to a cooperative diffusion coefficient reflecting the concentration fluctuations due to the polyions and counterions, and D_s to slow concentration fluctuations having a large correlation length (≈ 100 nm). The existence of two diffusive modes in salt-free solutions of polyelectrolytes cannot be explained within the framework of the scaling approach as proposed by de Gennes and Odijk.

(Keywords: semidilute polyelectrolyte solutions; diffusion; dynamic light scattering)

INTRODUCTION

At present, great attention is being devoted to the structure and properties of polyelectrolytes. In the case of flexible polyelectrolytes, where the electrostatic interaction is screened by an added low-molecular-weight electrolyte, the chains behave similarly to flexible neutral macromolecules. The behaviour of such solutions has been adequately described in terms of the scaling theory[1]. The scaling relations thus derived have been verified by an analysis of quasielastically scattered light (QELS) from sodium polystyrene sulphonate (NaPSS) solutions[2].

A much more complicated situation arises if we want to describe the behaviour of polyelectrolyte solutions without an added low-molecular-weight electrolyte, where the electrostatic repulsive forces between polyions are weakly screened, and thus relatively long-range. In dilute solutions the highly charged polyelectrolyte chains are nearly fully stretched owing to strong electrostatic repulsions of the like charges localized along the macromolecular chain. For such a case, Lifson and Katchalsky[3] suggested the so-called cell-model theory, where macromolecules can be represented as rigid, uniformly charged rods, arranged more or less in parallel and forming a 'hexagonal structure'. The model, which disregards deviations from the fully stretched conformation, cannot be used in a description of the behaviour of polyelectrolytes at higher concentrations, where the screening of electrostatic interactions by means of co-ions cannot be neglected any more.

Several years ago, de Gennes *et al.*[4] used scaling concepts to take into account the concentration dependences in characteristic quantities of polyelectrolyte systems, without the added low-molecular-weight electrolyte. For polyelectrolytes with a flexible backbone, three concentration regimes were distinguished differing in the behaviour of polyions. At the lowest concentrations ($c \ll c_G^*$, where c_G^* is the concentration corresponding to the crystallization process), the polyelectrolyte chains are on the average widely separated and fully stretched. The average dimensions of macromolecules are proportional to the degree of polymerization. Above the concentration c_G^* the chains are still fully stretched, but cannot freely orient any more. Electrostatic interactions between the polyions may lead to a three-dimensional lattice. At high concentrations ($c \gg c_G^*$), considerable overlap between the chains in solution takes place, leading to a transient network with a characteristic correlation length ξ which decreases with increasing concentration as $c^{-1/2}$. Chain segments shorter than ξ are regarded as fully stretched; all electrostatic interactions over a contour distance longer than ξ are screened off by other chains.

Recently, Odijk[1] and Skolnick and Fixman[5] have developed a concept of the electrostatic persistence length L_e to describe a concentration-dependent flexibility of the polyelectrolyte chain. The total persistence length L_t of the chain is split up into an intrinsic part L_p, which would characterize the chain in the absence of charge interactions, and an electrostatic part L_e, which decreases with increasing concentration as c^{-1} (consequence of

* Present address: Laboratory of Biophysics, Institute of Experimental Physics, Slovak Academy of Sciences, Solovjevova 47, 043 53 Košice, Czechoslovakia
† To whom correspondence should be addressed

0032-3861/87/060873-08$03.00

counterion screening of the charges on the macromolecule). This theory made possible a more exact description of the behaviour of polyelectrolytes without added salt, especially in the concentration range $c > c_G^*$. Odijk has introduced a critical concentration c^*, at which $L_t \simeq l$, where l is the contour length of the polyion. Three concentration regimes are now considered for $c > c_G^*$: (i) $c_G^* < c < c^*$, where $L_t > l$, and polyions are rigid rods arranged in a three-dimensional lattice; (ii) $c^* < c < c^{**}$ (c^{**} is defined as the concentration at which the lattice melts), where $L_t \gg \xi$, the three-dimensional lattice is deformed but preserves some anisotropy, and $\xi \sim c^{-1/2}$; (iii) $c^{**} < c$, where $L_t \ll \xi$, and the system is in the isotropic phase of worm-like chains (basically, two more concentration regimes can be distinguished for the cases where $L_t \simeq L_e$ or $L_t \simeq L_p$, respectively).

Odijk's theory was qualitatively supported by n.m.r. relaxation measurements[6], sedimentation measurements[7], SANS[8,9], SAXS[10], and static light-scattering experiments[11], spin-echo neutron scattering experiments[12,13] and QELS measurements[14-18]. In spite of this, however, quite a few unsolved problems still remain, such as the existence and behaviour of the slow mode relaxation times observed in QELS experiments at concentrations above c^*.

In this study we report QELS experiments performed with aqueous solutions of weak poly(methacrylic acid) (PMA), in the concentration range $c > c^*$. This system has been selected because of the possibility of varying the charge per unit length of the macromolecule, and thus also of electrostatic interactions by varying the degree of neutralization α of the acid in solution by means of a suitable alkali. We investigated the dependences of the diffusion coefficients and of the corresponding amplitudes of scattering intensities on α and c, with the aim of elucidating the character of dynamic processes in the system. Our experimental results are the first QELS data for weak polyelectrolyte acid solutions.

EXPERIMENTAL

Aqueous solutions were prepared using two PMA samples having molecular weight $M_w = 3.0 \times 10^4$ (PMA 1) and 4.0×10^5 (PMA 2), obtained by radical polymerization. Polydispersity of the samples determined from the QELS measurements[19] was $M_w/M_n = 2$ (PMA 1) and $M_w/M_n = 1.5$ (PMA 2—fractionated sample). The solutions were prepared using deionized water; the degrees of neutralization of PMA were adjusted by using sodium hydroxide. For the QELS measurements, a series of PMA solutions was prepared having various degrees of neutralization α, from $\alpha = 0$ to $\alpha = 1$ (α was determined potentiometrically). Prior to measurement, the samples were filtered through a glass bacterial filter G5 (Jena), or centrifuged. All measurements were carried out at 26°C.

Quasielastically scattered light was analysed by means of a homodyne spectrometer with a 96-channel digital correlator[20]. A He–Ne laser (model 125A, Spectra Physics) and an Ar laser (model ILA 120-1, Carl Zeiss, Jena) were the light sources.

Since the observed correlation functions $G(\tau)$, especially for solutions with $\alpha = 1$, were highly non-exponential, composite correlation functions covering a wide dynamic range (typically, from 0.5 μs to 1 s) were constructed on the basis of measurements at various sampling times, which provided a more complete view of the dynamics of polyelectrolyte solutions. These functions were analysed by the multiexponential linear programming method[21], which allowed us to determine a distribution function of decay times $A(\tau)$. In those cases where the distribution function $A(\tau)$ can be reduced to two main separated narrow bands, the double-exponential forced fit was used in the form

$$G(\tau) = \left[A_f \exp\left(-\frac{\tau}{\tau_{cf}} \right) + A_s \exp\left(-\frac{\tau}{\tau_{cs}} \right) \right]^2 + B \qquad (1)$$

where τ_{cf} and τ_{cs} are the fast and slow decay times, respectively, A_f and A_s are the respective scattering amplitudes, τ is the delay time and B is a constant. The simple correlation curves were force-fitted by a single exponential.

RESULTS

Dependence of the dynamic behaviour of PMA solutions on the degree of neutralization

Figure 1 shows typical results of measurements of the composite correlation functions $G(\tau)$ of PMA 1 solution for different α at $c = 36.6\ \mathrm{g\,l^{-1}}$. The limiting case $\alpha = 0$ represents an undissociated PMA solution; the case $\alpha = 1$ represents a fully dissociated solution (which corresponds to a solution of a strong polyelectrolyte without the added low-molecular-weight electrolyte). By using a multi-exponential fit, it was found that the distribution function $A(\tau)$ corresponding to these correlation curves may be adequately reduced to two main separated narrow bands centred at the fast time, τ_{cf} ($\sim 1\ \mu$s), and the slow time, τ_{cs} ($\sim 10^3$–$10^4\ \mu$s) (cf. *Figure 2*). For these reasons, the double-exponential forced fit was mainly used in the analysis of $G(\tau)$. No significant changes in the correlation function and in the fitting parameters could be detected for a measurement repeated after a few weeks.

The dynamic processes (fast and slow) characterized by the times τ_{cf} and τ_{cs} both have a diffusive character, because both τ_{cf}^{-1} and τ_{cs}^{-1} are linearly dependent on the square of the scattering vector q. Hence for the description of the dynamic behaviour of polyelectrolyte solutions, two diffusion coefficients, D_f ($= \tau_{cf}^{-1} q^{-2}$) and D_s ($= \tau_{cs}^{-1} q^{-2}$), may be introduced. Their values and the corresponding scattering amplitudes, A_f and A_s, are functions of α and c.

Figure 3 shows the dependences of D_f and D_s on α for PMA 1 ($c = 36.6\ \mathrm{g\,l^{-1}}$), obtained from the $G(\tau)$ functions in *Figure 1* by the double-exponential forced fit. The ratio

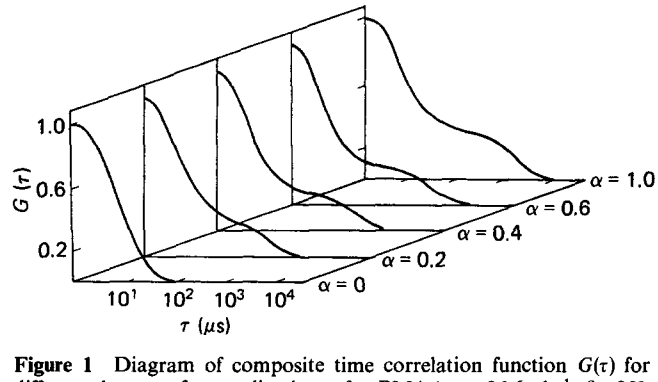

Figure 1 Diagram of composite time correlation function $G(\tau)$ for different degrees of neutralization α for PMA 1, $c = 36.6\ \mathrm{g\,l^{-1}}$, $\theta = 90°$

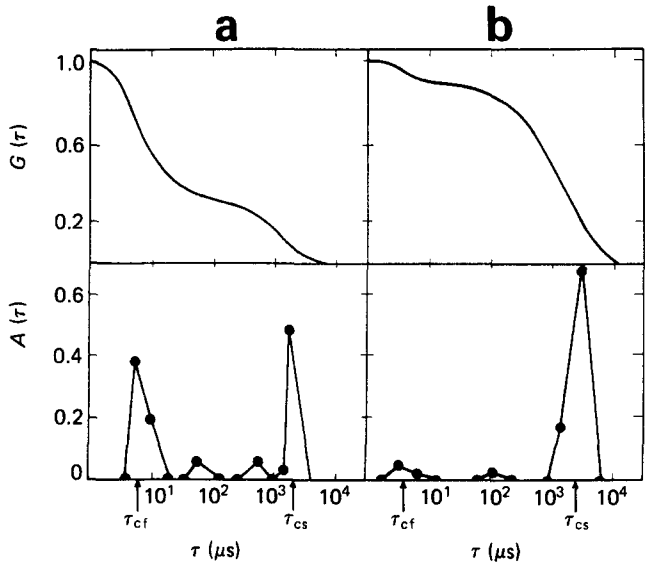

Figure 2 Composite time correlation functions $G(\tau)$ and corresponding distribution functions of decay times $A(\tau)$: (a) PMA 1, $c=36.6\,g\,l^{-1}$, $\alpha=1$, $\theta=90°$; (b) PMA 2, $c=1.9\,g\,l^{-1}$, $\alpha=1$, $\theta=90°$

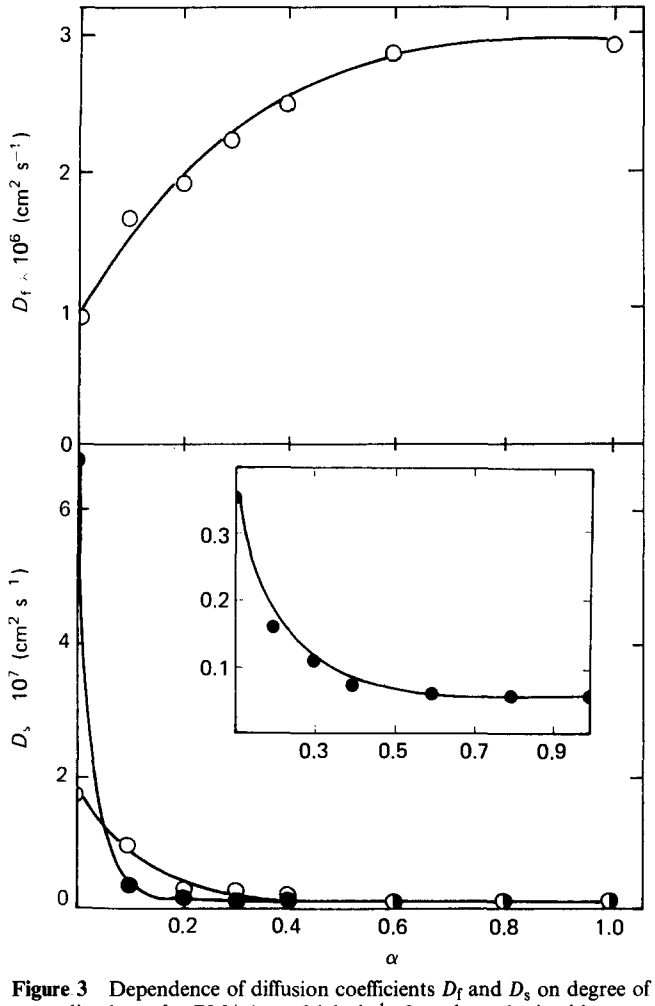

Figure 3 Dependence of diffusion coefficients D_f and D_s on degree of neutralization α for PMA 1, $c=36.6\,g\,l^{-1}$: ○, values obtained by two-exponential forced fitting to composite time correlation functions; ●, values obtained by single-exponential forced fitting to simple time correlation functions. (The meaning of these symbols remains unchanged also in the following figures)

of the scattering amplitudes A_s/A_f can be seen in *Figure 4*. Along with the composite correlation curves, simple correlation curves obtained with very short and very long sampling times were also analysed by the single-exponential forced fit. The agreement between the results obtained by employing both procedures is satisfactory for D_s with the exception of small α values (cf. *Figure 3b*). However, the short-sampling-time experiments do not provide satisfactory results for D_f.

In *Figure 3* it can be seen that, for $0<\alpha<0.4$, the original and virtually single diffusion mode is split into two: D_f increases and D_s decreases with increasing α. For $\alpha>0.4$, both diffusion coefficients are nearly independent of α. A similar behaviour has been observed for A_s/A_f: up to $\alpha=0.4$ it increases, then remains constant. The non-zero value of A_s/A_f for $\alpha=0$ is a consequence partly of the polydispersity of the sample PMA 1 itself ($M_w/M_n=2$) and partly of the weak dissociation of PMA, which makes α not exactly zero.

A similar situation has also been observed for the high-molecular-weight sample PMA 2, with the difference that the contribution of the fast mode to the total intensity of the scattered light is much smaller than in the case of PMA 1 (cf. *Figure 2b*, $A_s/A_f=20$). The weakness of the fast diffusion mode (D_f) impeded the obtaining of reliable data on its behaviour. *Figure 5* shows only the D_s vs. α dependence obtained by an analysis of simple correlation functions measured with long sampling times.

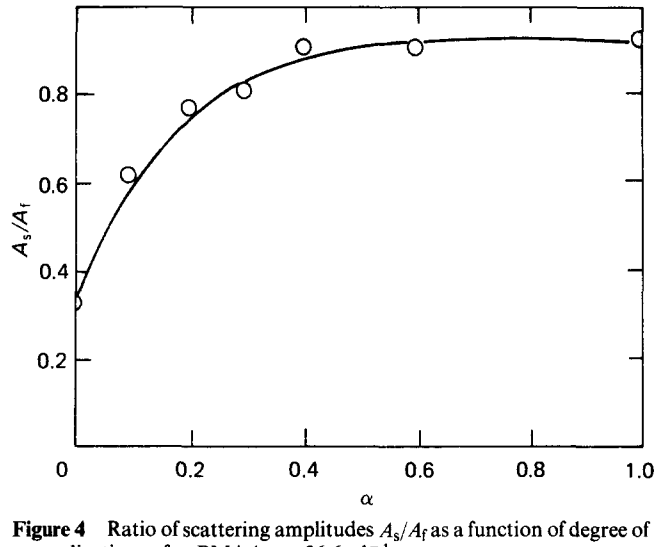

Figure 4 Ratio of scattering amplitudes A_s/A_f as a function of degree of neutralization α for PMA 1, $c=36.6\,g\,l^{-1}$

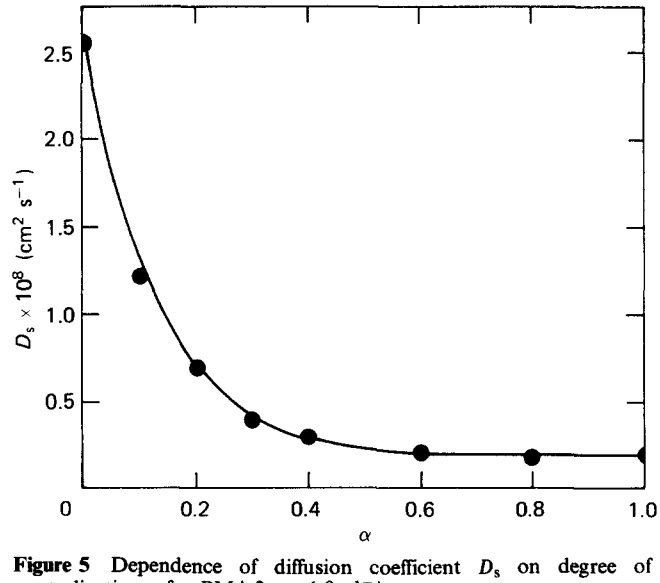

Figure 5 Dependence of diffusion coefficient D_s on degree of neutralization α for PMA 2, $c=1.9\,g\,l^{-1}$

Dependence of the dynamic behaviour of PMA solutions on concentration at $\alpha = 1$

From both PMA polymers a series of samples was prepared with concentrations ranging between $c = 0.33$ and $45\,g\,l^{-1}$. *Figure 6* shows composite correlation functions $G(\tau)$ of PMA 1 solutions for different concentrations ($\alpha = 1$). Within the whole concentration range under investigation, $G(\tau)$ could again be successfully fitted by two exponentials. In *Figure 7* we can see the dependences of D_f and D_s on c in logarithmic coordinates for PMA 1. The D_f value increases; that of D_s decreases with increasing concentration. In the vicinity of $c = 10\,g\,l^{-1}$, the increase in D_f ceases and for $c > 10\,g\,l^{-1}$

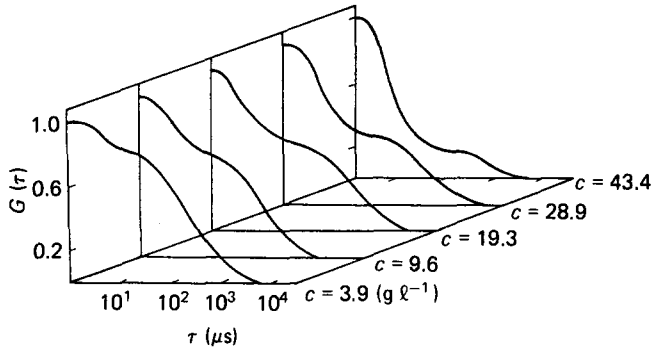

Figure 6 Diagram of composite time correlation function $G(\tau)$ for different concentrations for PMA 1, $\alpha = 1$

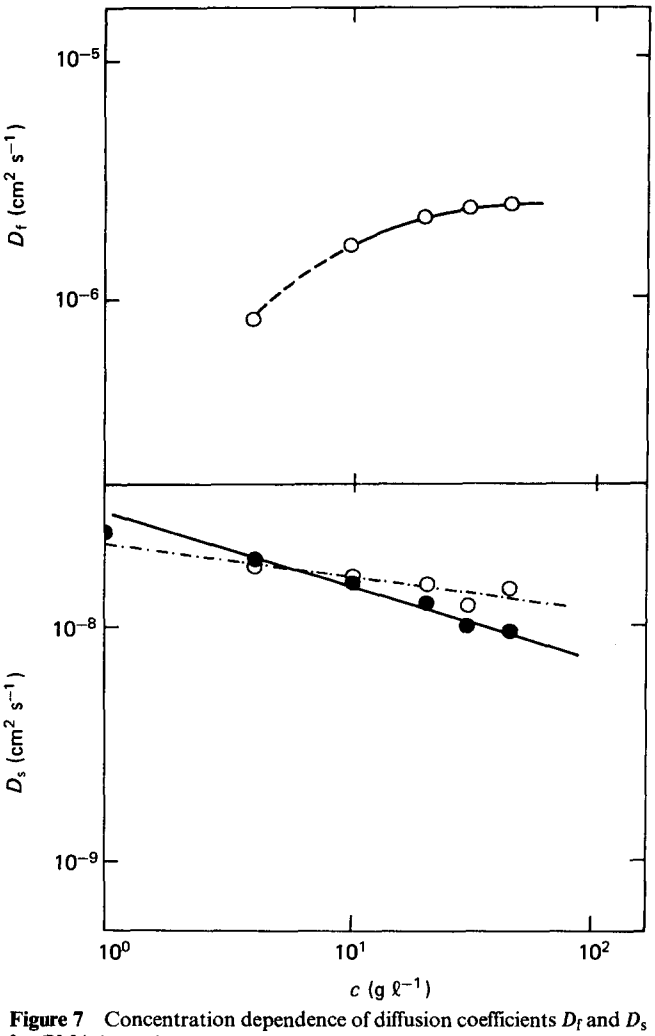

Figure 7 Concentration dependence of diffusion coefficients D_f and D_s for PMA 1, $\alpha = 1$

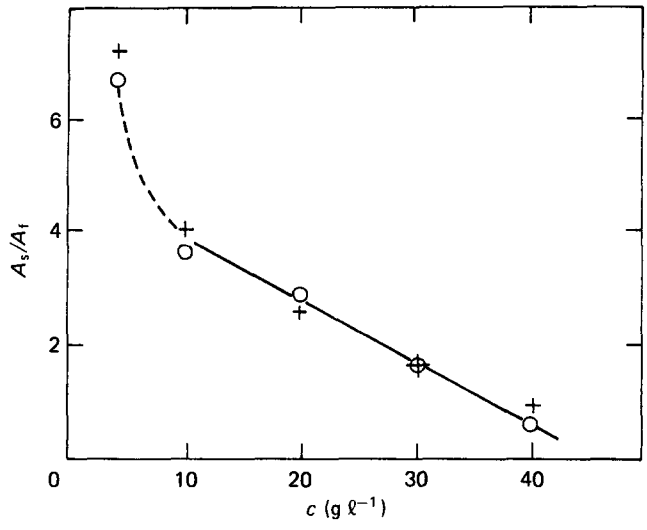

Figure 8 Dependence of A_s/A_f on concentration c for PMA 1, $\alpha = 1$: +, values obtained by the multiexponential linear programming method

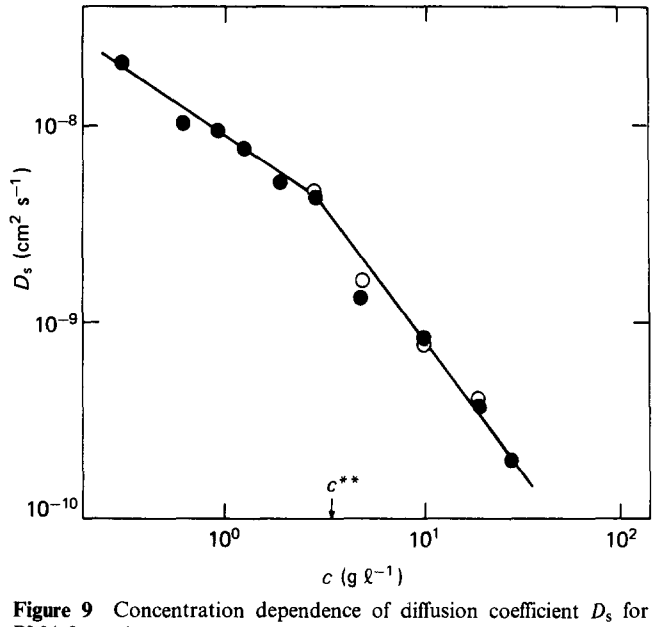

Figure 9 Concentration dependence of diffusion coefficient D_s for PMA 2, $\alpha = 1$

D_f becomes virtually independent of c. The dependence of D_s on c is comparatively weak ($\sim c^{-0.3}$) and linear in the coordinates used. The ratio of scattering amplitudes is plotted as a function of c in *Figure 8*. As has been demonstrated by model measurements with binary mixtures, at high A_s/A_f values the amplitudes cannot be determined reliably. In *Figure 8* this finding is reflected in the different curves drawn through the experimental points (full curve, reliable values; broken curve, less reliable values). With decreasing c the fast mode becomes less distinct, and below $c = 4\,g\,l^{-1}$ it can be detected only with difficulty (cf. *Figure 8*, $A_s/A_f > 7$).

With the polymer PMA 2, the dependence of D_f on c could not be reliably determined even at higher concentrations, because A_f/A_s still remained too low. the log–log plot of the D_s vs. c dependence at $\alpha = 1$ for PMA 2 can be seen in *Figure 9*. A distinctly different feature of this dependence compared with that in *Figure 7b* is a discontinuity near $c = 4\,g\,l^{-1}$, where the exponent of the concentration dependence changes from -0.7 to -1.4.

By comparing the results obtained for PMA 1 ($M_w = 3.0 \times 10^4$) and PMA 2 ($M_w = 4.0 \times 10^5$), we may

also evaluate, at least qualitatively, the effect of molecular weight on the dynamic behaviour of polyelectrolytes. The relative contribution of the slow mode to the total intensity of scattered light increases with increasing molecular weight (cf. *Figure 2*). For $c<4\,g\,l^{-1}$, the D_s vs. c dependence is weak in both cases, and even the D_s values lie close to each other. More pronounced differences between the two samples can be noticed for $c>4\,g\,l^{-1}$, where the drop in D_s with increasing c observed with PMA 2 sample occurs much more quickly than with PMA 1.

DISCUSSION

Before discussing experimental results, it is useful to outline the regimes of the concentration studied.

The onset of formation of ordered three-dimensional structures may be expected around values of c_G^* defined[4] by

$$c_G^*\,(g\,l^{-1}) \simeq 10^3 M_w/N_A l^3 \qquad (2)$$

in which N_A is the Avogadro number. For PMA, the magnitude of l is approximately given by the relation[22]

$$l\,(cm) \simeq 2.5\times10^{-8} M/M_m \qquad (3)$$

where M and M_m are molecular weights of the macromolecule and of the monomer unit, respectively. For PMA 1 and PMA 2, from (2) and (1) we obtain $l=87$ nm, $c_G^*\simeq 7.6\times10^{-2}\,g\,l^{-1}$ and $l=1163$ nm, $c_G^*\simeq 4.3\times10^{-4}\,g\,l^{-1}$ respectively. All the concentrations studied are higher than c_G^*, and even higher than c^* defined by Odijk[1] in the form

$$c^*\,(g\,l^{-1}) \simeq 10^3 (16\pi Q A l)^{-1} M_m/N_A \qquad (4)$$

where $Q=e^2/\varepsilon kT$ (in water at 25°C, $Q=7\times10^{-8}$ cm) is the Bjerrum length (e is the elementary charge and ε is the relative permittivity of water) and $A=l/Z$ is the contour distance between two successive charges along the macromolecular chain, which bears Z of them in total (for PMA, $A=2.5\times10^{-8}\alpha^{-1}$ cm). From (4), for PMA 1 we obtain $c^*\simeq 1.9\times10^{-1}\,g\,l^{-1}$, and for PMA 2 $c^*\simeq 1.4\times10^{-2}\,g\,l^{-1}$.

An important critical concentration is c^{**}, at which melting of the three-dimensional lattice takes place. Odijk's prediction for c^{**} is given by

$$c^{**}\,(g\,l^{-1}) \simeq 10^3 (100\pi Q^2 A)^{-1} M_m/N_A \qquad (5)$$

which is a concentration independent of M and l, and for PMA $c^{**}\simeq 3.7\,g\,l^{-1}$.

For concentrations $c>c^*$, with increasing c the radius R of a single coil decreases owing to increasing flexibility of the polymer chain ($L_e\sim c^{-1}$). For $c^*<c<c^{**}$, R decreases as $c^{-1/2}$, i.e. more quickly than the average spacing d between macromolecules ($\sim c^{-1/3}$)[1]. In the case of macromolecules with low molecular weights and above a certain critical concentration, denoted by c^x, a situation may occur where $d>2R$. From the condition $d/2R\simeq 1$ and using the theoretical concentration dependence for R (relation (34) in ref. 1), we obtain

$$c^x\,(g\,l^{-1}) \simeq 10^3 N (16\pi Q)^{-3} M_m/N_A \qquad (6)$$

where N is the number of monomer units in a macromolecular chain. The theoretical function $R(c)$ can only be applied if N (or M or l) is so low that for c^x the inequality $c^*<c^x<c^{**}$ holds. This occurs, for example, with PMA 1, where $c^x\simeq 1.1\,g\,l^{-1}$.

For concentrations $c>c^{**}$, R still decreases, but more slowly than d; $R\sim c^{-5/16}$ (for $L_t\simeq L_e$) or $R\sim c^{-3/16}$ (for $L_t\simeq L_p$)[1]. At high concentrations, polymer coils may again overlap.

Such somewhat speculative reasonings may also be supported by experimental results obtained by means of SANS experiments with mixtures of normal and labelled (deuterated) PMA polymers[23]. Thus, for a sample with $M_w=2.1\times10^4$ at $c=40\,g\,l^{-1}$ and $\alpha=1$, the radius of gyration $R_G=7.5$ nm was determined, which is much lower than $l=59$ nm[23]. At a given c, such polymer coils overlap only a little ($d/2R_G\sim 0.6$—surroundings of the overlap concentration). With respect to the assumed weak concentration dependence of R_G above c^{**} ($L_e<L_p$ at $c=40\,g\,l^{-1}$)[23], it may be expected that, near c^{**}, $d>2R_G$. Our PMA 1 sample differs in molecular weight only a little from that described above, so that analogous behaviour may be anticipated.

For the structure of a low-molecular-weight solution, one may expect that for $c>c^*$ it approaches that of dispersions of interacting charged particles, i.e. a solid-like or liquid-like spatial arrangement. The c^{**} value calculated from (5) assuming hexagonal structure does not obviously fit in with reality for low-molecular-weight polyelectrolyte samples. It is corroborated by the finding that the ordering of low-molecular-weight polyelectrolytes is observed also at $c=40\,g\,l^{-1}$ ($\sim 11\,c^{**}$)[9,10].

The calculated critical concentrations, along with the molecular parameters, are given for both polymers in *Table 1*.

On summarizing all these findings, it may be said that for both samples the QELS measurements were carried out in the concentration ranges $c^*<c<c^{**}$ and $c>c^{**}$. Moreover, the concentrations used for sample PMA 1 were larger than c^x.

Dependence of the diffusion coefficients on the degree of neutralization

Experimental results show that the diffusion coefficient D_f of the sample PMA 1 increases (cf. *Figure 3a*) while D_s decreases for both samples (cf. *Figures 3b* and *5*) with increasing α. The largest changes of both coefficients take place in the range from $\alpha=0$ to $\alpha=0.4$, while at higher α

Table 1 Molecular parameters of PMA samples and critical concentration of their aqueous solutions for $\alpha=1$ calculated from equations (2), (4), (5) and (6)

Sample	M_w	l (nm)	N	c_G^* (g l^{-1})	c^* (g l^{-1})	c^{**} (g l^{-1})	c^x (g l^{-1})
PMA 1	3.0×10^4	87	349	7.6×10^{-2}	1.9×10^{-1}	3.7	1.1
PMA 2	4.0×10^5	1163	4651	4.3×10^{-4}	1.4×10^{-2}	3.7	

they are very small. Other characteristic quantities of PMA solutions behave similarly: for example, the radius of gyration of polyions, R_G, increases with increasing α and reaches a steady value near $\alpha = 0.5$[23]. A similar dependence has also been observed for q_{max} (wavevector corresponding to the maximum intensity of scattered radiation) in SANS[9] and SAXS[10] experiments.

The relatively large changes of the measured quantities of PMA solutions in the range from $\alpha = 0$ to 0.4 are obviously due to the quickly increasing number of charged groups on the polyion, $Z\ (=eN\alpha)$, which brings about increase of inter- and intramolecular electrostatic interactions. The lack of sensitivity of the measured values to changes in α above $\alpha = 0.4$ can be accounted for by the condensation of counterions, which takes place at $\alpha > \alpha_M$; for monovalent counterions, α_M corresponds to a situation where $Q/A = 1$[22]. For PMA, $\alpha_M \simeq 0.36$, which is a value close to the values $\alpha = 0.4$–0.5 above which the measured quantities become independent of α. For $\alpha > \alpha_M$, the charge density on polyions is stabilized, and so are the electrostatic interactions.

The existence of slow and fast modes in QELS experiments performed with solutions of charged macromolecules has already been demonstrated several times for systems other than the one investigated in this study. A slow diffusion process has been observed with strong polyelectrolyte solutions at low concentrations of a low-molecular-weight salt in the so-called 'extraordinary region'. The very first results were obtained with solutions of poly(L-lysine)[24]; later results were recorded using systems such as aqueous solutions of DNA[25–27] and NaPSS[17,18]. In all these systems an increase in the salt concentration in solution was accompanied by the so-called extraordinary–ordinary phase transition when the slow diffusion process suddenly disappears. An analogous transition has in fact been observed also by us, for weak polyelectrolytes with decreasing α, the only difference being that the transition is a continuous one and virtually ends only at $\alpha = 0$ (cf. *Figures 3*, *4* and *5*).

Fast diffusion process. For $\alpha = 0$, the solution of PMA 1 can be regarded as dilute for all concentrations studied, which means that D_f more or less corresponds to the diffusion of free polymer coils. Hence, the apparent hydrodynamic radius $R_{H,app}$ determined from D_f by using the Stokes–Einstein law should be close to the hydrodynamic radius of the polymer coil. For $c = 36.6\ g\ l^{-1}$, we have $R_{H,app} = 3.3$ nm. This value may be compared with the R_G value obtained by SANS measurements[23] for a similar PMA sample. For PMA having $M_w = 2.1 \times 10^4$, at $\alpha = 0$ and $c = 40\ g\ l^{-1}$, $R_G = 4.47$ nm is reported, which is virtually identical with the unperturbed radius of gyration. Assuming that $R_G \sim M^{1/2}$, we obtain for PMA 1 $R_G = 5.3$ nm. The ratio $\rho = R_G/R_{H,app} = 1.6$ is close to the theoretical value $\rho = 1.504$ reported[28] for linear polymers at the θ temperature.

For $\alpha > 0$, D_f also represents the diffusion coefficient of polyions. The increase in D_f with increasing α may be explained by an interaction with counterions. In the coupled-mode theory[29], D_f for $\alpha > 0$ corresponds to the Nernst–Hartley diffusion coefficient, D_{NH}; the diffusion coefficient D_{NH} of the large polyion is increasingly higher than its hydrodynamic value as Z increases.

For the sample PMA 2, the fast mode for $\alpha > 0$ corresponds to the cooperative diffusion coefficient, which reflects the concentration fluctuations due to polyions and counterions.

Slow diffusion process. The slow mode is slower by several orders of magnitude than the fast one. The origin of this mode has not yet been completely elucidated. In the literature it is correlated either with the reptation mode[15], or with the diffusion process of interchain domains (clusters)[16] having relatively large dimensions. To distinguish these cases experimentally, the angular dependences of A_f/A_s and D_s were measured for the sample PMA 1 (cf. *Figures 10a* and *10b*). In the case of the reptation mode it may be expected, with respect to the small dimensions of the molecules themselves, that both scattering amplitudes are virtually angle-independent. In the latter case, the size of the domains should be reflected in the angular dependences of both quantities. The results in *Figure 10a* evidently support the other variant of the interpretation. Since the measurements were carried out at $qR_G \ll 1$, it may be assumed that A_f is angle-independent, and the main effect in *Figure 10a* is due to the angular dependence of A_s. To estimate the size of the domains, we calculated from data in *Figure 10* values of the apparent radius of gyration, $R^{(d)}_{G,app}$, on the assumption that the scatterers are isolated particles; in the small-angle limit we obtain $R^{(d)}_{g,app} = 47$ nm (at $c = 9.4\ g\ l^{-1}$ and $\alpha = 1$). This assumption is not strictly valid for the observed domains. Therefore, the calculated $R^{(d)}_{G,app}$ values are not equal to the real domain size, but they may be used as an estimate of the domain size only.

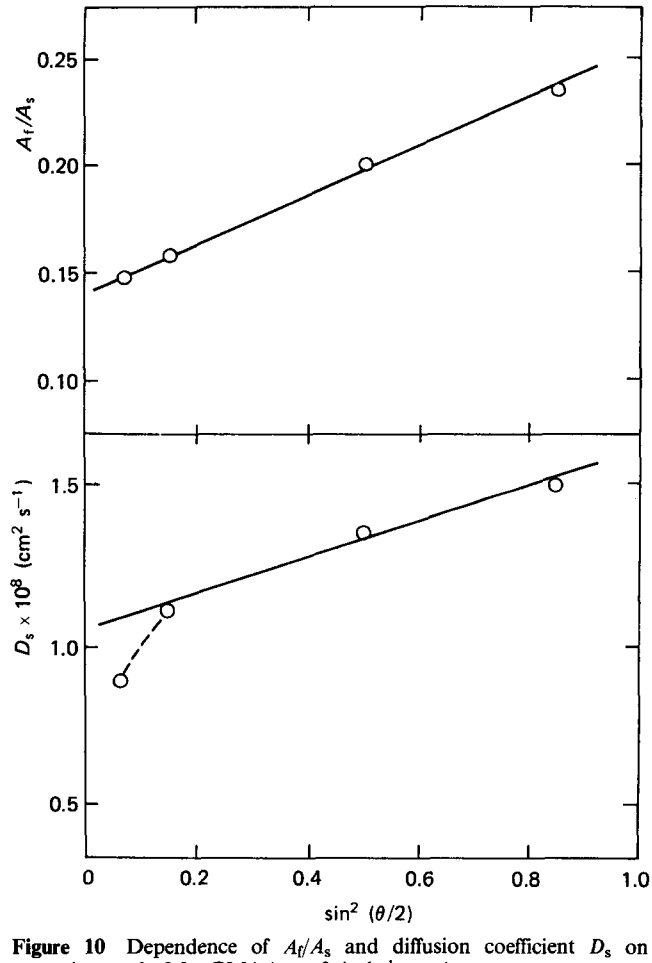

Figure 10 Dependence of A_f/A_s and diffusion coefficient D_s on scattering angle θ for PMA 1, $c = 9.4\ g\ l^{-1}$, $\alpha = 1$

Similarly, $R_{G,app}^{(d)}$ of the domains may be estimated from the angular dependence of D_s (cf. *Figure 10b*). From the theory derived for isolated particles in the small-angle limit, we obtain[30]:

$$D(q)=D_0[1+C(R_{G,app}^{(d)}q)^2] \qquad qR_{G,app}^{(d)}\leqslant 1 \qquad (7)$$

where D_0 is the diffusion coefficient in the limit $q\rightarrow 0$, and C is a characteristic constant that depends on the architecture of scatterers; its values vary from 0.133 (solid spheres) to 0.2 (polycondensates)[30]. Using these extreme C values, we obtain $50\,nm < R_{G,app}^{(d)} < 65\,nm$. Hence, $R_{G,app}^{(d)}$ obtained from both measurements is $\sim 50\,nm$.

As far as we know, no similar data for flexible polyions have been reported, but clusters of similar dimensions have been detected at low salt concentrations in tRNA solutions[31] ($M_w \simeq 2.65\times 10^4$).

Thus, the slow mode observed with PMA 1 is due to the diffusion of domains consisting of a major number of macromolecules and having dimensions close to 50 nm. The formation of such domains cannot be explained within the framework of an isotropic model suggested by de Gennes[4] and Odijk[1]. On the other hand, however, the results obtained do not contradict the three-dimensional two-phase model suggested by Ise[32], according to which regions having an ordered structure (domains) are formed in the polyelectrolyte solution, while the remaining part of the solution is in a disordered state.

Preliminary results of integral light-scattering measurements performed with the PMA 2 sample also show a pronounced angular dissymmetry. For $c=2\,g\,l^{-1}$, a procedure analogous to that employed with the sample PMA 1 gave $R_{G,app}^{(d)}\simeq 100\,nm$[33]. In agreement with the authors of ref. 16 we believe that the slow mode can be correlated to slow concentration fluctuations of large domains.

The polyelectrolyte concentration dependence of diffusion coefficients

The D_f value of the PMA 1 sample increases with increasing concentration (cf. *Figure 7a*): above $c=10\,g\,l^{-1}$, D_f is virtually concentration-independent. The lower D_f value observed for $c=3.6\,g\,l^{-1}$ is already not very reliable, because of the high A_s/A_f value.

The concentration independence of D_f above c^{**} is also suggested by the results of QELS[15,16] and neutron spin-echo experiments[12,13] using aqueous solutions of NaPSS without added salt.

The concentration dependence of D_s for $c<c^{**}$ is not pronounced for both PMA samples. For aqueous solutions of NaPSS (extraordinary region), D_s has been declared as concentration-independent[15,16], which does not basically contradict the results obtained with PMA. Both samples differ in the concentration dependence of D_s above c^{**}, however. While in the case of PMA 1 the character of the concentration dependence virtually does not change at the concentration c^{**}, a clear discontinuity is observed with PMA 2 (cf. *Figures 7b* and *9*). Such results only corroborate the view that c^{**} calculated from (5) does not correspond to reality for low-molecular-weight polyelectrolytes. Changes in the concentration dependence similar to those observed with PMA have also been found for high-molecular-weight samples of NaPSS[15,16]. According to our results, interpretation of such behaviour by using the reptation model proposed by Koene and Mandel[15] is purely speculative.

A decrease in the relative scattering intensity of the slow mode (cf. *Figure 8*) with increasing concentration observed with the sample PMA 1 may be explained qualitatively by a decrease in the number of domains in solution due to 'melting' of the structure. Basically, such a trend has also been observed for NaPSS solutions[15,16], where in agreement with our results the fast mode disappeared below c^{**}.

The increase in the contribution of the slow mode with increasing molecular weight to the total intensity of scattered light is also in accordance with measurements performed with other systems. One may agree with the view that, with moderate molecular weight and at a very low ionic strength, both diffusion modes can be observed[34].

CONCLUSION

The existence of two diffusion modes (D_f and D_s) in salt-free solutions of PMA and their dependence on α and c cannot be fully explained within the framework of the scaling theory as proposed by de Gennes[4] and Odijk[1]. Our results of concentration measurements performed with PMA 2 confirm that concentration regimes $c^*<c<c^{**}$ and $c>c^{**}$ exist in aqueous solutions of charged macromolecules in the absence of low-molecular-weight electrolyte, and can be detected by QELS experiments. A different interpretation of dynamic modes has been suggested for a sample with $M_w=3.0\times 10^4$ and $M_w=4.0\times 10^5$. In the former case, D_f can be attributed to the Nernst–Hartley diffusion coefficient, and D_s (based on angular measurements) (*Figure 9*) can be assigned to the diffusion interchain domains (clusters) having radius of gyration $R_G\simeq 50\,nm$. In the latter case, where a pronounced overlap of polymer coils must be considered, D_f probably corresponds to the cooperative diffusion coefficient, while D_s corresponds to slow concentration fluctuations having a large correlation length ($\simeq 100\,nm$).

REFERENCES

1 Odijk, T. *Macromolecules* 1979, **12**, 688
2 Koene, R. S., Nicolai, T. and Mandel, M. *Macromolecules* 1983, **16**, 220, 227, 231
3 Lifson, S. and Katchalsky, A. *J. Polym. Sci.* 1954, **13**, 43
4 de Gennes, P. G., Pincus, P., Velasco, R. M. and Brochard, F. *J. Physique* 1976, **37**, 1461
5 Skolnick, J. and Fixman, M. *Macromolecules* 1977, **10**, 944
6 Levij, M., de Bleijser, J. and Leyte, J. C. *Chem. Phys. Lett.* 1982, **87**, 34
7 Roots, J. and Nyström, B. *Polymer* 1981, **22** 573
8 Nierlich, M., Williams, C. E., Boué, F., Cotton, J. P., Daud, M., Farnoux, B., Jannink, G., Picot, C., Moan, M., Wolff, C., Rinaudo, M. and de Gennes, P. G. *J. Physique* 1979, **40**, 701
9 Pleštil, J., Mikeš, J., Dušek, K., Ostanevich, Yu. M. and Kuchenko, A. G. *Polym. Bull.* 1981, **4**, 225
10 Pleštil, J., Mikeš, J. and Dušek, K. *Acta Polym.* 1979, **30**, 29
11 Drifford, M. and Dalbiez, J. P. *J. Phys. Chem.* 1984, **88**, 5368
12 Hayter, J., Jannink, G., Brochard, F. and de Gennes, P. G. *J. Physique Lett.* 1980, **41**, L451
13 Nallet, F., Jannink, G., Hayter, J., Oberthür, R. and Picot, C. *J. Physique* 1983, **44**, 87
14 Grüner, F., Lehmann, W. P., Fahlbuch, H. and Weber, R. *J. Phys. A* 1981, **14**, L307
15 Koene, R. S. and Mandel, M. *Macromolecules* 1983, **16**, 973
16 Drifford, M. and Dalbiez, J. P. *J. Physique* 1985, **46**, L311
17 Drifford, M., Dalbiez, J. P., Tabti, K. and Tirant, P. *J. Chim. Phys.* 1985, **82**, 571
18 Drifford, M. and Dalbiez, J. P. *Biopolymers* 1985, **24**, 1501

19 Štěpánek, P., Tuzar, Z. and Koňák, Č., 'Physical Optics of Dynamic Phenomena and Processes in Macromolecular Systems', (Ed. B. Sedláček), Walter de Gruyter, Berlin and New York, 1985, p. 461
20 Koňák, Č, Štěpánek, P. and Sedláček, B. *Czech. J. Phys. A* 1984, **34**, 497
21 Zimmermann, K., Delay, M. and Licinio, P. *J. Chem. Phys.* 1985, **82**, 2228
22 Manning, G. S. *J. Chem. Phys.* 1969, **51**, 934
23 Pleštil, J., Ostanevich, Yu. M., Bezzabotov, V. Yu., Hlavatá, D. and Labský, J. *Polymer* 1986, **27**, 839
24 Lin, S. C., Lee, W. I. and Schurr, J. M. *Biopolymers* 1978, **17**, 1041
25 Fulmer, A. W., Julyek, A., Benbasat, A. and Bloomfield, V. A. *Biopolymers* 1981, **20**, 1147
26 Schmitz, K. S. and Lu, M. *Biopolymers* 1984, **23**, 797
27 Schmitz, K. S., Lu, M., Singh, N. and Ramsay, D. J. *Biopolymers* 1984, **23**, 1637
28 Yamakawa, H., 'Modern Theory of Polymer Solutions', Harper and Row, New York, 1971
29 Berne, B. J. and Pecora, R., 'Dynamic Light Scattering', John Wiley, New York, 1976
30 Burchard, W. *Adv. Polym. Sci.* 1983, **48**, 1
31 Patkowski, A., Gulari, E. and Chu, B. *J. Chem. Phys.* 1980, **73**, 4178
32 Ise, N., Okubo, T., Yamamoto, K., Kawai, H., Hashimoto, T., Fujimura, M. and Hiragi, Y. *J. Am. Chem. Soc.* 1980, **102**, 7901
33 Sedlák, M., Koňák, Č. and Dušek, K., to be published
34 Schmitz, K. *Biopolymers* 1984, **22**, 2169